P H Y S I C A L   R E V I E W   L E T T E R S

Two-Dimensional Bose Gases near Resonance: Competing Two-Body and Three-Body Effects

Mohammad S. Mashayekhi,[1] Jean-Sébastien Bernier,[1] Dmitry Borzov,[1] Jun-Liang Song,[2] and Fei Zhou[1]

[1]*Department of Physics and Astronomy, University of British Columbia, Vancouver V6T 1Z1, Canada*
[2]*Institute for Quantum Optics and Quantum Information, Austrian Academy of Sciences, A-6020 Innsbruck, Austria*

We report in this Letter the results of our investigation of 2D Bose gases beyond the dilute limit emphasizing the role played by three-body scattering events. We demonstrate that a competition between three-body attractive interactions and two-body repulsive forces results in the chemical potential of 2D Bose gases to exhibit a maximum at a critical scattering length beyond which these quantum gases possess a negative compressibility. For larger scattering lengths, the increasingly prominent role played by three-body attractive interactions leads to an onset instability at a second critical value. The three-body effects studied here are universal, fully characterized by the effective 2D scattering length a_{2D} (or the size of the 2D bound states) and are, in comparison to the 3D case, independent of three-body ultraviolet physics. We find, within our approach, the ratios of the contribution to the chemical potential due to three-body interactions to the one due to two-body to be 0.27 near the maximum of the chemical potential and 0.73 in the vicinity of the onset instability.

Two-dimensional quantum many-body systems have been, for many years, a subject of fascination for condensed matter and nuclear physicists alike. More recently, this topic also caught the attention of the cold atom community with the realization of quantum Bose gases confined to two-dimensional geometries [1–4]. These experimental studies have so far explored these cold atom systems at temperatures close to the Berezinskii-Kosterlitz-Thouless phase transition [5–7]. They highlighted the loss of long-range order due to the proliferation of vortices above the transition temperature, and the existence of two-dimensional quasicondensates with algebraic long-range order and long wavelength thermal fluctuations below the transition. However, the fundamental properties of 2D Bose gases near absolute zero, where quantum effects are dominant, have yet to be addressed. In particular, on both theoretical and experimental sides, very little work has been carried out to study 2D Bose gases near resonance. The main purpose of this Letter is to provide new light on the properties of 2D Bose gases in this limit.

Compared to 3D Bose gases near resonance, which received more attention in recent years [8–11], 2D gases possess important advantages. First, the ratio between elastic and inelastic collision cross sections can be significantly enhanced when atoms are confined to two-dimensional traps [12]. Second, in 2D, trimers and few-body structures are all universal as the absolute energy scale of the spectrum is uniquely set by the two-body binding energy and is independent of the short distance property of three-body interactions [13–16]. This is distinctly different from the physics of Efimov states in 3D as, in this case, the absolute energy scale is set by the ultraviolet physics of three-boson scatterings [17].

These advantages are related to the dramatic suppression of the low energy effective interactions and phase shifts by coherent interference in 2D Bose gases. Most previous works on these gases considered systems where the range of the repulsive interactions or the core size of the hardcore bosons, a_0, were much smaller than the interparticle distances [18–20]. The results of these studies are only applicable when $\frac{1}{\ln(na_0^2)}$ (n is the density of bosons) is much smaller than unity, a limit corresponding to dilute gases in 2D. Here, we focus on the physics of 2D Bose gases prepared on the upper branch and interacting via a resonating contact interaction. In other words, we are interested in the thermodynamics of metastable Bose gases beyond the Popov-Schick dilute regime [18,19]. Such a setup can be achieved experimentally through a combination of Feshbach resonance and optical confinement [21–24]. Theoretically, to study 2D near-resonance Bose gases, we introduce a 2D effective scattering length a_{2D}. This new tuning parameter is defined as the position of the node in the wave function for two scattering particles and is also identified as the size of the two-body bound state. In general, a_{2D} can be tuned to values larger than the averaged interatomic distance and can even be infinite.

Our study of 2D Bose gases at large scattering lengths unveils that near resonance the properties of these gases are primarily dictated by the competition between three-body attractive interactions and two-body repulsive forces. We also show that the energetics of 2D Bose gases near resonance are universal as they only depend on the parameter na_{2D}^2. Finally, we investigate the behavior of the chemical potential for a wide range of scattering lengths. We find that the chemical potential first increases with a_{2D} but very quickly reaches a maximum at $\frac{1}{\ln(na_{2D}^2)} = -0.135$ beyond

which the Bose gas develops a negative compressibility. Increasing a_{2D} further brings about an onset instability at $\frac{1}{\ln(na_{2D}^2)} = -0.175$. We identify both critical values to result from the important role played by three-body attractive interactions. Within our approach, we can estimate the contributions from three-body interactions to the two-body ones to be around 0.27 near the maximum of chemical potential and 0.73 in the vicinity of the onset instability.

To carry out this study of 2D Bose gases, we employ a method previously developed to understand the physics of 3D Bose gases near resonance [25,26]. In this approach, the chemical potential of noncondensed particles, μ, and the density of condensed atoms, n_0, are first introduced as given parameters. The Hamiltonian describing such a condensate interacting with noncondensed atoms through a short range interaction is

$$H = \sum_{\mathbf{k}} (\epsilon_{\mathbf{k}} - \mu) b_{\mathbf{k}}^{\dagger} b_{\mathbf{k}} + 2U_0 n_0 \sum_{\mathbf{k}} b_{\mathbf{k}}^{\dagger} b_{\mathbf{k}}$$
$$+ \frac{1}{2} U_0 n_0 \sum_{\mathbf{k}} b_{\mathbf{k}}^{\dagger} b_{-\mathbf{k}}^{\dagger} + \frac{1}{2} U_0 n_0 \sum_{\mathbf{k}} b_{\mathbf{k}} b_{-\mathbf{k}}$$
$$+ \frac{U_0}{\sqrt{S}} \sqrt{n_0} \sum_{\mathbf{k'},\mathbf{q}} b_{\mathbf{q}}^{\dagger} b_{\mathbf{k'}+\frac{\mathbf{q}}{2}} b_{-\mathbf{k'}+\frac{\mathbf{q}}{2}} + \text{H.c.}$$
$$+ \frac{U_0}{2S} \sum_{\mathbf{k},\mathbf{k'},\mathbf{q}} b_{\mathbf{k}+\frac{\mathbf{q}}{2}}^{\dagger} b_{-\mathbf{k}+\frac{\mathbf{q}}{2}}^{\dagger} b_{\mathbf{k'}+\frac{\mathbf{q}}{2}} b_{-\mathbf{k'}+\frac{\mathbf{q}}{2}} + \text{H.c.} \quad (1)$$

Here, $\epsilon_{\mathbf{k}} = \hbar^2 \mathbf{k}^2/2m$, the sum is over nonzero momentum states, S is the total area, and U_0 is the strength of the bare short range interaction. Later, we will evaluate n_0 and μ self-consistently as a function of the 2D scattering length, a_{2D}, and of the total density n.

Once the full system energy density $E(n_0, \mu)$ is known, one can calculate μ_c, the chemical potential for the condensed atoms, and $n - n_0$, the density of noncondensed atoms. This step is achieved using the following thermodynamic relations:

$$\mu_c = \frac{\partial E(n_0, \mu)}{\partial n_0}, \quad n = n_0 - \frac{\partial E(n_0, \mu)}{\partial \mu}; \quad \mu = \mu_c(n_0, \mu).$$
$$(2)$$

As hinted above, in the ground state, one requires μ_c, the chemical potential for the condensed atoms, to be equal to the chemical potential μ. This equilibrium condition, first emphasized in Ref. [27], yields a self-consistent equation. The evaluation of $E(n_0, \mu)$ for a given μ and n_0 is usually carried out diagrammatically [27,28]. To capture the role of three-body interactions and to compare it with two-body contributions, we restrict ourselves to the virtual processes involving only two or three excited atoms. Truncating the Hilbert space accordingly, we can then sum up all connected diagrams contributing to the energy density. Within this truncation scheme, only the irreducible two- and three-body effective interaction potentials $g_{2,3}$ appear in the final expression for $E(n_0, \mu)$. In order to implement the

self-consistency condition and simplify the computation of $E(n_0, \mu)$, we introduce for the noncondensed or virtual atoms an additional parameter $\eta = \Sigma - \mu$, where $\Sigma(n_0, \mu)$ is the self-energy. Physically, η can be understood as an energy shift due to the interaction between condensed and noncondensed atoms. Using the same series of diagrams as in our study of 3D Bose gases near resonance [25], but carrying out the calculations in two spatial dimensions, we obtain for the energy density

$$E(n_0, \mu) = \frac{1}{2} n_0^2 g_2(2\eta) + \frac{1}{3!} n_0^3 \text{Re } g_3(3\eta) + \cdots$$

with $\quad g_2(2\eta) = \frac{\hbar^2}{m} \frac{4\pi}{\ln\frac{B_2}{2\eta}},$

$$g_3(3\eta) = 6g_2^2(2\eta) g_3^*(3\eta), \quad (3)$$

where $g_3^*(3\eta) = \frac{\hbar^2}{m} \int \frac{4q\,dq}{2\eta + q^2} \frac{G_3'(-3\eta, q)}{\ln\frac{B_2}{3q^2/4+3\eta}}.$

$g_{2,3}$ stand for, respectively, the *renormalized* two- and three-body interactions in a condensate. We will discuss this point in more details below. $G_3'(-3\eta, p)$ represents the three-atom off shell scattering amplitude (corresponding to the sum of all N-loop contributions with $N = 1, 2, 3, \dots$). G_3' is the solution to the following integral equation, where $\hbar$ and m were exceptionally set to unity to improve readability:

$$G_3'(-3\eta, p) = \int \frac{4q\,dq}{\ln\frac{B_2}{3q^2/4+3\eta}} \frac{1}{\sqrt{(3\eta + p^2 + q^2)^2 - (pq)^2}}$$
$$\times \left(\frac{-1}{2\eta + q^2} - G_3'(-3\eta, q) \right). \quad (4)$$

Note that in Eqs. (3) and (4), $B_2 = \Lambda \exp(\frac{4\pi\hbar^2}{U_0 m})$, where Λ is an energy cutoff related to the effective interaction range, R^*, via $\Lambda = \frac{\hbar^2}{mR^{*2}}$. As $B_2 = \frac{\hbar^2}{ma_{2D}^2}$, $g_{2,3}$ are uniquely determined by the parameter $\frac{n\hbar^2}{mB_2}$ or na_{2D}^2.

For repulsive interactions (or positive U_0), B_2 is larger than Λ and so a_{2D} is bounded from above by the interaction range R^*. When U_0 is infinite (hardcore potential), a_{2D} is equal to the core size a_0. For attractive interactions (or negative U_0), the case we focus on here, B_2 is precisely the dimer binding energy, and a_{2D} is the size of the bound state and can well exceed R^*. As a consequence, na_{2D}^2, the fundamental tuning parameter for $E(n_0, \mu)$, can take values larger than unity. The gas can hence be tuned away from the dilute limit [29].

Before detailing our results, we need to mention, as a matter of completeness, that as $E(n_0, \mu)$ explicitly depends on $\Sigma(n_0, \mu)$, n_0, and μ, Eqs. (2) and (3) are supplemented by the relation

$$\Sigma(n_0, \mu) = \mu_c(n_0, \mu) + \frac{\partial \mu_c}{\partial \ln n_0}, \qquad (5)$$

an extension of Hugenholtz-Pines theorem [27].

Three-dimensional counterparts to Eqs. (2), (3), and (5), were used in Ref. [25] to obtain the chemical potential of 3D Bose gases near resonance. These self-consistent equations provided highly precise estimates for the chemical potential in the dilute limit. Near resonance, this approach predicted a maximum in the chemical potential and an accompanied onset instability. These features were fully consistent with the conclusions drawn from a renormalization-group equation approach [26]. This first study concluded that in 3D the dominating contribution to the chemical potential came from irreducible two-body interactions; for cold atoms, the three-body contribution was negligible. For 2D Bose gases, the story is very different: three-body interactions play a more important role as seen on Fig. 1.

To analyze the contribution coming from the three-body effect, we first solve Eqs. (2) and (3) excluding the contribution of g_3, and obtain the chemical potential solely due to two-body interactions [see Fig. 1 dashed red line]. Here, g_2 is defined as the effective two-body interaction renormalized by scattering events off condensed atoms and includes a subset of N-body interactions defined in the vacuum [30]. Neglecting g_3 interactions, the self-consistent equations take the simple form

$$\tilde{\mu} = \frac{4\pi}{\ln\frac{1}{2\alpha\tilde{\mu}}} + \frac{8\pi^2}{\tilde{\mu}\ln^3\frac{1}{2\alpha\tilde{\mu}}}, \qquad \frac{1}{\tilde{n}_0} = 1 + \frac{2\pi}{\tilde{\mu}}\frac{1}{\ln^2\frac{1}{2\alpha\tilde{\mu}}}, \qquad (6)$$

where $\tilde{\mu} = \frac{m\mu}{\hbar^2 n_0}$, $\tilde{n}_0 = \frac{n_0}{n}$, and $\alpha = n_0 a_{2D}^2$ [31]. The solution of Eq. (6) in the limit of small α is

$$\mu = \frac{n}{m}\frac{4\pi\hbar^2}{\ln\frac{1}{\alpha}}\left(1 - \frac{1}{\ln\frac{1}{\alpha}}[\ln|\ln\alpha| - \ln 4\pi + C] + \cdots\right), \qquad (7)$$

where $C = \ln\frac{1}{2}$ within this self-consistent approach. This solution, valid in the dilute limit, agrees well with previous studies [18,19,32]. Another solution with μ approaching $\frac{\hbar^2}{ma_{2D}^2}$ exists in this limit but is unstable. As α or na_{2D}^2 is increased, the dilute gas solution approaches this higher energy unstable solution, and at the critical value $na_{2D}^2 = 1.42 \times 10^{-2}$, the two solutions coalesce into one. Beyond this point, no real solution to Eq. (6) exists revealing the presence of an instability. The basic structure sketched here, when three-body contributions are neglected, is qualitatively the same as that of 3D Bose gases: μ is maximum when an onset instability sets in and for larger na_{2D}^2, develops an imaginary part implying the formation of molecules.

We now turn our attention to the contribution of $g_3(3\eta)$. $g_3(3\eta)$ is obtained by first numerically solving Eq. (4) for $G_3'(-3\eta, p)$ and then by carrying out the integral involving $G_3'(-3\eta, q)$ in Eq. (3). The result of this procedure is shown in Fig. 2 where we plot $g_3^*(3\eta)$. We chose to plot $g_3^*(3\eta)$ and not $g_3(3\eta)$ as the former is not cluttered by trivial effects due to $g_2^2(2\eta)$. We identify two kinds of resonant scattering processes defining the basic structure of $g_3(3\eta)$. The first one is a three-body resonance between three condensed atoms with zero energy and a dimer plus a noncondensed atom with total energy $3\eta - B_2$. Here, 3η is the mean-field energy shift due to the exchange interaction between the noncondensed atom-dimer structure and the condensate. This leads to the first peak (from left to right) at $3\eta = B_2$. The second process is a three-body resonance between three condensed atoms and a trimer with either
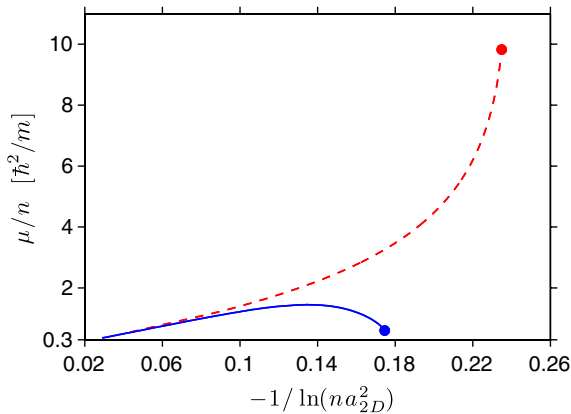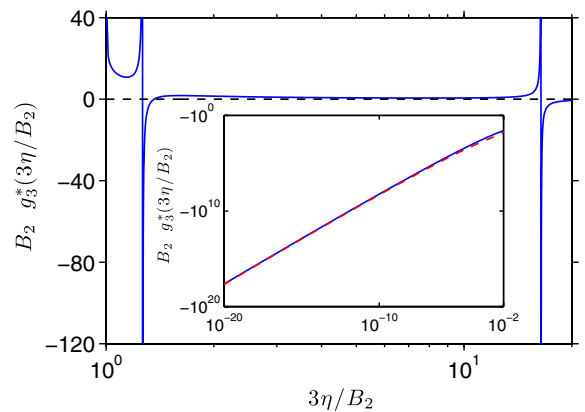

FIG. 1 (color online). The chemical potential, in units of $\frac{\hbar^2 n}{m}$, as a function of na_{2D}^2. The dashed (red) line is the solution of the self-consistent equation when only two-body interactions are included. The solid (blue) line is the solution when both two- and three-body interactions are included. This figure highlights that the behavior of the chemical potential is drastically altered by three-body physics.

FIG. 2 (color online). Three-body interaction g_3^* [defined in Eq. (3)] as a function of the energy shift $\eta = \Sigma - \mu$; η is determined self-consistently together with μ. Inset: full and two-loop behavior of g_3^* for small η values [respectively, solid (blue) and dashed (red) lines]. For $\frac{3\eta}{B_2} < 1$, the numerical integration over the momentum was done from 0 to $50\frac{\sqrt{B_2 m}}{\hbar}$.

binding energy $B_3^{(1)}$ or $B_3^{(2)}$ (or total energies $3\eta - B_3^{(1)}$ or $3\eta - B_3^{(2)}$). This process produces the second and third peaks at $3\eta = B_3^{(1,2)}$. We find numerically that $B_3^{(1)} = 1.296B_2$ and $B_3^{(2)} = 16.643B_2$. These energies are fully consistent with the results of previous studies exploring the physics of three-body bound states [13,14,33]. Unlike in 3D where a logarithmically large number of Efimov states exist, in 2D there are only two trimer states. Remarkably, their energies are uniquely determined by B_2 without involving an additional three-body parameter, a fascinating feature emphasized in Refs. [13,14].

The effect of three-body scatterings on the quantum gas is mainly determined by the property of g_3 when η is relatively small. We checked numerically that in the limit of very small η, g_3 can be well fitted by an attractive interaction of the scaling form

$$\frac{\hbar^4}{2m^2\eta} \frac{1}{\ln^2 \frac{B_2}{2\eta} \ln^2 \frac{B_2}{3\eta}},$$

capturing the dominant two-loop contribution [34] (see Fig. 2). Including the contribution due to three-body physics in the evaluation of the chemical potential results in two main effects. First, due to the attractive tail of g_3 in the small η limit, as shown in Fig. 3, the
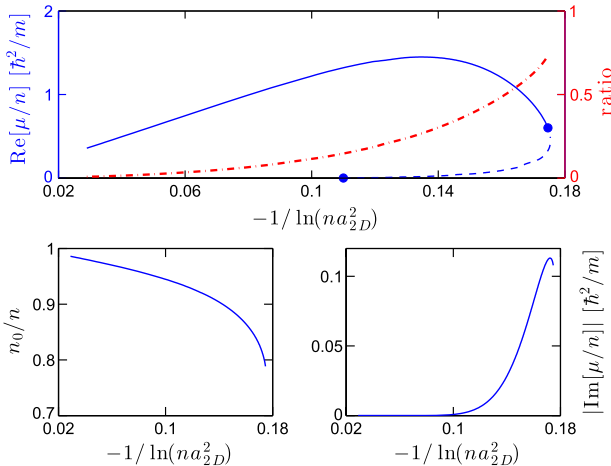

FIG. 3 (color online).   Top panel: ratio between the contributions of three-body and two-body interactions as a function of na_{2D}^2 (dash-dotted red line) and chemical potential for 2D Bose gases (solid blue line). An additional metastable solution (dashed blue line) also exists when g_3 is included. The maximum value of μ is $1.45\frac{\hbar^2 n}{m}$ and occurs at $na_{2D}^2 = 0.604 \times 10^{-3}$. Bottom left panel: condensation fraction n_0/n as a function of na_{2D}^2. Bottom right panel: imaginary part of the chemical potential when taking into account the contribution of all three-body recombination processes. Note that $|\text{Im}\mu| \ll \text{Re}\mu$ for all considered na_{2D}^2, indicating the quasistatic nature of the Bose gases. Hence, three-body recombination plays very little role in our energetic analysis and can be safely neglected for the range of parameters considered.

instability is shifted away from $na_{2D}^2 = 1.42 \times 10^{-2}$ and occurs at a much smaller value of $na_{2D}^2 = 3.26 \times 10^{-3}$ [35]. At this new instability point, the chemical potential is dramatically reduced, from $9.82\frac{\hbar^2 n}{m}$ to $0.601\frac{\hbar^2 n}{m}$ when g_3 is included. In other words, the three-body effective interaction further destabilizes the quantum gas. The second and equally important effect is that the inclusion of three-body interactions results in the appearance of a maximum in the chemical potential at $na_{2D}^2 = 0.604 \times 10^{-3}$ before the onset instability occurs. The maximum value of the chemical potential is $\mu_{\max} = 1.45\frac{\hbar^2 n}{m}$ and the condensation fraction at the maximum is 91%.

Between the maximum and instability points, the quantum gas exhibits a negative compressibility and can potentially collapse into a high density phase. Although the fate of the Bose gases with negative compressibilities and the details of the corresponding dynamics are beyond the scope of our investigation, we speculate that in this regime a quantum gas eventually fragments into the droplet matter discussed in Ref. [14]. In 3D, the instability originated from a shift of the dimers due to scatterings off condensates and was a precursor of the sign change of the effective two-body interaction g_2 [26]. For 2D Bose gases, the situation is completely different. Here, the instability is a consequence of the competition between the repulsive two-body interaction (positive g_2) and the attractive three-body interaction (negative g_3) in the low energy limit. For a 2D Fermi gas, the Pauli blocking effect was recently demonstrated to lead to an instability at a finite scattering length [23].

We also plot in Fig. 3 the relative weight of the three- to two-body contributions to the chemical potential. As anticipated, the three-body contribution is negligible in the dilute limit when $na_{2D}^2 \ll 1$ but quickly becomes important as na_{2D}^2 is increased. The prominent role played by three-body scattering leads to a maximum in the chemical potential before the instability point. At this maximum, the ratio between the three- and two-body contributions reaches 0.27. The shift of the instability is caused by the attractive three-body interactions.

In conclusion, we demonstrated that the properties of 2D Bose gases at large scattering lengths or near resonance are dictated by three-body effects. We showed that the contributions of trimer states are universal as they only depend on the effective two-body scattering length, a_{2D}, and not on the short distance properties of three-body interactions, an aspect unique to 2D Bose gases. Our results also suggest the existence of strong correlations in the three-atom channel near resonance. This feature remains to be probed experimentally.

[1] Z. Hadzibabic, P. Krüger, M. Cheneau, B. Battelier, and J. Dalibard, Nature (London) **441**, 1118 (2006).

[2] V. Schweikhard, S. Tung, and E. A. Cornell, Phys. Rev. Lett. **99**, 030401 (2007).

[3] P. Cladé, C. Ryu, A. Ramanathan, K. Helmerson, and W. D. Phillips, Phys. Rev. Lett. **102**, 170401 (2009).

[4] C.-L. Hung, X. Zhang, N. Gemelke, and C. Chin, Nature (London) **470**, 236 (2011).

[5] V. L. Berezinskii, Sov. Phys. JETP **34**, 610 (1972).

[6] J. M. Kosterlitz and D. J. Thouless, J. Phys. C **6**, 1181 (1973).

[7] N. D. Mermin and H. Wagner, Phys. Rev. Lett. **17**, 1133 (1966).

[8] S. B. Papp, J. M. Pino, R. J. Wild, S. Ronen, C. E. Wieman, D. S. Jin, and E. A. Cornell, Phys. Rev. Lett. **101**, 135301 (2008).

[9] S. E. Pollack, D. Dries, M. Junker, Y. P. Chen, T. A. Corcovilos, and R. G. Hulet, Phys. Rev. Lett. **102**, 090402 (2009).

[10] N. Navon, S. Piatecki, K. Günter, B. Rem, T. C. Nguyen, F. Chevy, W. Krauth, and C. Salomon, Phys. Rev. Lett. **107**, 135301 (2011).

[11] R. J. Wild, P. Makotyn, J. M. Pino, E. A. Cornell, and D. S. Jin, Phys. Rev. Lett. **108**, 145305 (2012).

[12] Z. Li and R. V. Krems, Phys. Rev. A **79**, 050701 (2009).

[13] L. W. Bruch and J. A. Tjon, Phys. Rev. A **19**, 425 (1979).

[14] H. W. Hammer and D. T. Son, Phys. Rev. Lett. **93**, 250408 (2004).

[15] E. Nielsen, D. V. Fedorov, and A. S. Jensen, Few-Body Syst. **27**, 15 (1999).

[16] D. Blume, Phys. Rev. B **72**, 094510 (2005).

[17] V. Efimov, Phys. Lett. **33B**, 563 (1970); Sov. J. Nucl. Phys. **12**, 589 (1971).

[18] M. Schick, Phys. Rev. A **3**, 1067 (1971).

[19] V. N. Popov, Theor. Math. Phys. **11**, 565 (1972).

[20] D. S. Fisher and P. C. Hohenberg, Phys. Rev. B **37**, 4936 (1988).

[21] D. S. Petrov and G. V. Shlyapnikov, Phys. Rev. A **64**, 012706 (2001).

[22] I. Bloch, M. Dalibard, and W. Zwerger, Rev. Mod. Phys. **80**, 885 (2008).

[23] V. Pietilä, D. Pekker, Y. Nishida, and E. Demler, Phys. Rev. A **85**, 023621 (2012).

[24] L.-C. Ha, C.-L. Hung, X. Zhang, U. Eismann, S.-K. Tung, and C. Chin, following Letter, Phys. Rev. Lett. **110**, 145302 (2013).

[25] D. Borzov, M. S. Mashayekhi, S. Zhang, J.-L. Song, and F. Zhou, Phys. Rev. A **85**, 023620 (2012).

[26] F. Zhou and M. Mashayekhi, Ann. Phys. (Amsterdam) **328**, 83 (2013).

[27] N. M. Hugenholtz and D. Pines, Phys. Rev. **116**, 489 (1959).

[28] S. T. Beliaev, Sov. Phys. JETP **7**, 289 (1958); **7**, 299 (1958).

[29] For a quasi-two-dimensional cold gas near Feshbach resonance, a_{2D} is a function of l_0, the confinement radius along the perpendicular direction, and of the free space scattering length a_{3D}. For shallow 2D bound states, $a_{2D} = \sqrt{\frac{\pi}{0.915}} l_0 \exp(-\sqrt{\frac{\pi}{2}} \frac{l_0}{a_{3D}})$ [21–23].

[30] In the dilute limit, g_2 reproduces the most dominating contribution; the residue effects are from the irreducible $N = 4, 6, \ldots$-body interactions and are parametrically smaller than the contributions from g_2, i.e., smaller by a factor of $\frac{1}{\ln(na_{2D}^2)}$. See also similar discussions on 3D cases in Ref. [25].

[31] In obtaining this equation, we take into account Eq. (5) and set $\partial\eta/\partial\mu = 1$, $\partial\eta/\partial n_0 = g_2$, and $\eta = \mu$ to simplify the structure.

[32] S. R. Beane, Phys. Rev. A **82**, 063610 (2010).

[33] H. W. Hammer and D. T. Son further argued in Ref. [14] that there exists fascinating 2D N-body *bound* states with $N(>3)$ finite but smaller than a critical value. These few-body states, obtained by only taking into account two-body interactions, are mesoscopic droplets; the spatial extent of which becomes *exponentially small* when the number of atoms N is much larger than two. Experimentally, these proposed bound state solutions might be potentially explored on the *lower branch* near resonance, but not on the *upper branch*, the scattering channel we are interested in. In addition, in 3D, attractive bosons on the lower branch have been experimentally explored and turned out to be very unstable. The lower branch states in this limit can be partially described by an early theory in P. Nozières and D. Saint-James, J. Phys. (Paris) **43**, 1133 (1982). Here, our theoretical study focuses instead on the many-body physics of scattering atoms with a uniform density. This topic was not explored in Ref. [14] nor in the references mentioned above.

[34] A diagrammatic calculation similar to the one presented in Ref. [25] suggests that the leading N-loop contributions to g_3 for small values of η/B_2 are $g_3^{(N\text{-loop})} = C_N \frac{\hbar^4}{2m^2\eta} \frac{1}{\ln^2\frac{B_2}{2\eta}\ln^N\frac{B_2}{3\eta}}$ with $N = 2, 3, 4\ldots$; the prefactor C_N can be computed numerically. For the most dominating two-loop contribution, $C_2 = -6.3 \times 10^3$.

[35] The onset instability found without three-body effects occurs at a density similar to that observed in a variational Monte Carlo study using a Jastrow-type trial wave function [36]. On the other hand, the critical value of na_{2D}^2 obtained, when taking into account three-body effects, is one order of magnitude smaller than the value obtained in the previously cited variational study.

[36] S. Pilati, J. Boronat, J. Casulleras, and S. Giorgini, Phys. Rev. A **71**, 023605 (2005).